Calibration and Validation of XY Micropositioners with Vision.

Ning Tan, Cédric Clévy, Guillaume J. Laurent, Nicolas Chaillet

Calibration and Validation of $XY\Theta$ Micropositioners with Vision

Ning Tan, Cédric Clévy, Guillaume J. Laurent, and Nicolas Chaillet

***Abstract*— Accuracy is very important criterion for micro-manipulation systems, especially for microassembly. In this paper, we propose a full procedure of kinematic calibration and validation for $XY\Theta$ micropositioners, which are used as coarse positioning in our microassembly platform. Based on vision, two methods (self-calibration and classical calibration) are presented, implemented, tested and compared. The differential evolution (DE) algorithm is applied to identify the kinematic parameters. After calibrations, we perform tests of accuracy and repeatability through controlling the micropositioners via inverse kinematics.**

I. INTRODUCTION

Microassembly has become a critical technology in the micro and nanotechnologies [1]. The increasing needs for microsystems conduct to the development of new concepts and skilled microassembly cells. Performing efficient microassembly tasks require high accurate microrobots and control schemes[2]. Kinematic calibration is a process concerning of locating the end-effector of the robot manipulator in a global coordinate frame with improved absolute accuracy by identifying inaccurate and unknown geometric parameters [3], [4]. Large amount of calibration methods have been proposed for improving the accuracy of robots and machine tools [5], [6]. However, most of them are focusing on macroscale robots (e.g., industrial robots) while less article discussed such a topic for microrobots. Meanwhile, the need for high performances microrobots and microrobotic cells increases rapidly (e.g., in micro-assembly field) [1]. Hence, calibration strategies and measuring devices shall be adapted for small-sized robots and their compact workspace. High performance-cost rate devices would be given top priority. Here, two calibration methods are applied to the micropositioners. One is self-calibration (also called autonomous calibration) method through positioning the tool tip at a fixed point with different configurations. Another is classical method based on minimizing the difference between measured and calculated end-point positions.

In this paper, we propose a full procedure of calibration and validation for 3-DOF micropositioners $XY\Theta$ whose joint coordinates are known by integrated sensors. First, the principles of two calibration methods and identification algorithm are presented in Section II. Subsequently, we provide a vision-based metrology. Experiment setup and results for calibration and validation are shown in Section IV. The validation tests are done according to the requirements of ISO-9283 International standard [7]. This is followed by a conclusion in the last section.

N. Tan, C. Clévy, G. Laurent and N. Chaillet are with FEMTO-ST Institute, UMR CNRS-6174 / UFC / ENSMM / UTBM Automatic Control and Micro-Mechatronic Systems Department (AS2M Department), 25000 Besançon, France. ning.tan, cclevy, guillaume.laurent, nicolas.chaillet@femto-st.fr

TABLE I
TABLE OF DH PARAMETERS

i	α_i	a_i	θ_i	d_i
1	0	0	$\frac{\pi}{2}$	X
2	$\frac{\pi}{2}-\gamma$	0	$\frac{\pi}{2}$	Y
3	$\frac{\pi}{2}$	0	Θ	0

II. CALIBRATION

A. Modeling

We used Denavit-Hartenberg (DH) convention to model the micropositioners. Fig. 1 shows the relationship between all coordinate frames and locations of parameters to be identified. Here, $Ox_Ry_Rz_R$ is defined as robot global frame and $Ox_0y_0z_0$ as robot base frame. P is the tool tip whose positions are concerned. In Fig. 2, three kinematic parameters γ, L, τ to be identified are unknown, where γ is the differential angle between ideal perpendicular angle $\frac{\pi}{2}$ and real angle of X axis and Y axis; L is the distance from tool tip to the rotation center of Θ stage; τ is the direction angle relative to x axis. According to DH convention, the four DH parameters α_i, a_i, θ_i and d_i [3], [4], [8] are listed in Table I. It's worth pointing out that in this paper we focus on 2 dimensional space, so some parameters only contributing to vertical direction are neglected and set as zeros. As mentioned before, X, Y, Θ are known information by internal sensors. Therefore the only unknown parameter from link 1 to link 3 is γ.

Commonly, the location of reference frame i with respect to reference frame $i-1$ can be described by a homogeneous transformation matrix ${}^{i-1}T_i$. The homogeneous transformation of a rotation about an axis and a translation along an axis could be denoted by Rot_{axis} and $Trans_{axis}$, respectively. Hence, the transformation from robot base frame 0 to robot frame RF is expressed as:

$$ {}^{R}T_0 = Rot_y(\frac{\pi}{2})Rot_z(\frac{\pi}{2}). $$

The transformation from rotary positioner frame 3 to robot base frame 0 is calculated through concatenation of individual transformations according to Table I:

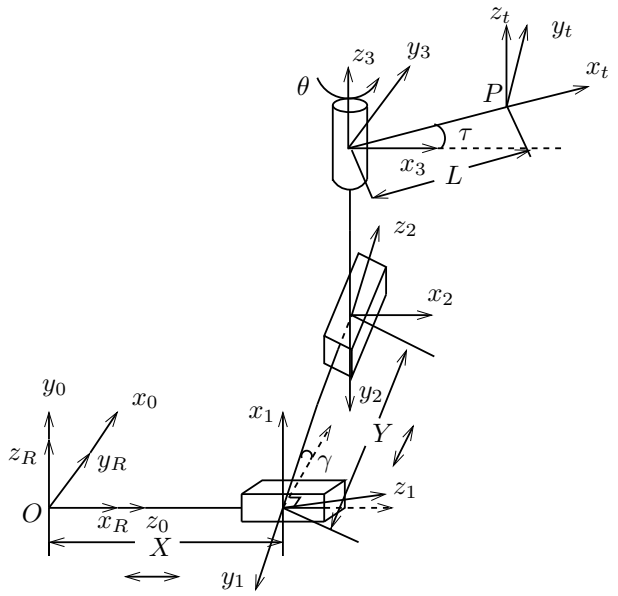

Fig. 1. Coordinate frames for calibration modeling.

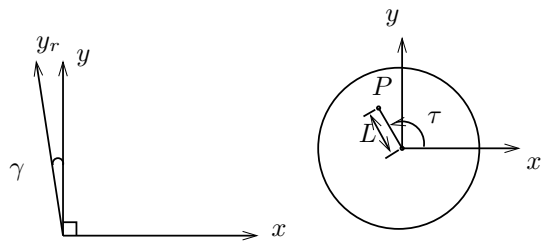

Fig. 2. Parameters to be identified

$$
\begin{aligned}
{}^0T_3 &= {}^0T_1\ {}^1T_2\ {}^2T_3 \\
&= Rot_z(\frac{\pi}{2})Trans_z(X)Rot_x(\frac{\pi}{2}-\gamma)Rot_z(\frac{\pi}{2}) \\
&\quad Trans_z(Y)Rot_x(\frac{\pi}{2})Rot_z(\Theta)
\end{aligned}
$$

Moreover, the tool tip frame t with respect to frame 3 is defined as

$$
{}^3T_t = Rot_z(\tau)Trans_x(L),
$$

where τ and L are orientation and position parameters of point of interest P in frame 3.

Consequently, the forward kinematics of the micropositioners is given by

$$
{}^RT_t = {}^R\ T_0\ {}^0T_3\ {}^3T_t.
$$

The position of the point of interest in planar dimension is

$$
\begin{aligned}
P &= [x_R, y_R], \\
x_R &= (c\gamma c\Theta + s\gamma s\Theta)Lc\tau + (s\gamma c\Theta - c\gamma s\Theta)Ls\tau \\
&+ X + Ys\tau, \\
y_R &= (c\gamma s\Theta - s\gamma c\Theta)Lc\tau + (s\gamma s\Theta - c\gamma c\Theta)Ls\tau \\
&+ Yc\tau,
\end{aligned}
$$

where P denotes the coordinate of the tool tip; c and s are the abbreviations of cos and sin operators.

Therefore, the coordinates of the tool tip in robot frame RF is the kinematic function of each pose (X, Y, Θ), which can be expressed as:

$$
P = f(q(X, Y, \Theta), \phi), \tag{1}
$$

where q is the correspondingly joint variables vector consisting of three joint coordinates X, Y and Θ; ϕ is the parameters vector to be identified.

B. Self-Calibration

The self-calibration method used imposes virtual single point constraint on the end-effector by positioning the tool tip at a fixed point with different poses using visual servo control. The internal sensors of the micropositioners record the coordinates of all poses at the fixed point.

The measurement procedure is as following:

1. Set rotation joint Θ as Θ_n, $n = 1, 2, \ldots, N$.

2. Visual servo controller positions the tool tip P to a fixed point within the tolerance in image frame, which is assumed a fixed point in robot frame as well, meanwhile records the corresponding measured by integrated encoders X_n and Y_n. Then, one pose measurement has collected and is expressed as $q_n(X_n, Y_n, \Theta_n)$.

3. Set the next rotation joint as $\Theta_{n+1} = \Theta_n + 5^\circ$ with stepsize 5°.

4. Follow the control scheme of step 2 and obtain measuring pose $q_{n+1}(X_{n+1}, Y_{n+1}, \Theta_{n+1})$

5. Similarly, total N measurements are obtained.

For arbitrary two poses $q_i(X_i, Y_i, \Theta_i)$ and $q_j(X_j, Y_j, \Theta_j)$, P^i is equal to P^j. Hence, ϕ can be identified by minimizing a cost function, which is defined as:

$$
E_{sel} = \sum_{n=1}^{3N(N-1)/2} \sqrt{\epsilon_{sel}(n)\epsilon_{sel}^T(n)}, \tag{2}
$$

where

$$
\epsilon_{sel} = \begin{bmatrix} P_c^1 - P_c^2 \\ P_c^1 - P_c^3 \\ \vdots \\ P_c^1 - P_c^N \\ P_c^2 - P_c^3 \\ \vdots \\ P_c^{N-1} - P_c^N \end{bmatrix}, \text{ with } 3N(N-1)/2 \text{ elements.}
$$

P_c is the calculated coordinate by using the calculated ϕ.

C. Classical Calibration

As comparison, we also performed classical calibration to the same micropositioners. What is different from self-calibration is identification algorithm need to find not only the kinematic parameters but also the relation parameters between the image and the robot frames. In this case, algorithm aims to minimize the difference between the calculated coordinates P_c and measured (or real) coordinates P_r. The cost function is:

$$E_{cla} = \sum_{n=1}^{N} \sqrt{\epsilon_{cla}(n)\epsilon_{cla}^{T}(n)}, \tag{3}$$

where

$$\epsilon_{cla} = \begin{bmatrix} P_c^1 - P_r^1 \\ P_c^2 - P_r^2 \\ \vdots \\ P_c^N - P_r^N \end{bmatrix}, \text{ with } 2N \text{ elements.}$$

D. Identification Algorithm

In this paper, the calibration problem is developed based on the kinematic equations of micropositioners, and then transformed into the optimization problem solved by Differential evolution (DE). DE shows especially efficient and robust for problems containing continuous variables [9], [10]. Error functions E_{sel} and E_{cla} in (2) and (3) are continuous, nonlinear, no-convex, and have several local minima. Therefore, the DE algorithm is used for identification of parameters in this research. DE is a population-based optimization algorithm, in which a candidate solution is called an individual and individuals constitute a population. The complete evolution goes through mutation, crossover, and selection operation. For optimization problem with m parameter variables, the individual is represented by parameter vector $\phi = (\phi_1, \phi_2, \cdots, \phi_m)$. Each generation of population G is represented as $\phi_{iG}, i = 1, 2, \cdots, M$, in which M is the population size. In mutation,

$$V_{i,G+1} = \phi_{r1,G} + F(\phi_{r2,G} - \phi_{r3,G}), \tag{4}$$

where $V_{i,G+1}$ is mutant vector generated after mutation, r_1, r_2, r_3 are mutually different random integer indices selected from $\{j | j \neq i, j \in [1, M]\}$. Step size $F \in [0, 2]$ is a real constant determining the amplification of the added differential variation. For crossover,

$$U_{i,G+1} = (U_{1i,G}, U_{2i,G}, \cdots, U_{ni,G})$$

$$U_{ji,G+1} = \begin{cases} V_{ji,G} \text{ if rand}b(j) \leq C_R \text{ or } j = rnbr(i) \\ \phi_{ji,G+1}, \text{ otherwise,} \end{cases} \tag{5}$$

where rand$b(j) \in$[0,1] is the jth evaluation of a norm random number, $C_R \in$[0,1] is the crossover constant set by the user, and $rnbr$(i) is an index randomly chosen from i dimensions to ensure that at least one parameter from the mutated vector $V_{i,G+1}$ can be attained. In selection stage,

$$\phi_{i,G+1} = \begin{cases} U_{i,G+1} \text{ if } J(U_{i,G+1}) < J(\phi_{i,G}) \\ \phi_{i,G}, \text{ otherwise,} \end{cases} \tag{6}$$

where J could be J_{sel} or J_{cla} depending on the calibration method used.

First, the initial population of DE is randomly generated. In every generation, mutation is employed according to (4) and crossover operation is implemented as (5). Then, based on the quality of $\phi_{i,G}$ and $U_{i,G+1}$, selection operation is carried out according to (6) and the selected individuals constitute the new population of the next generation.

III. VISION-BASED METROLOGY

The calibration and performance tests are based on CCD camera measurement assuming no image distortion and perfect parallelism between image plane and robot plane. For self-calibration, the locating of tool tip at a given point is done by visual servo control constructed by MATLAB/Simulink software.

A. Image Specification

The image format is 1024×768 mono and the frame rate is 7.5 fps. To determine the scale factor (μm-to-pixel rate), a preliminary experiment was performed [11], [12]. The micropositioners tracked the same rectangular path five times and a total of 5 sets of increments for the input (Δq) and output (Δw) displacements were recorded to calculate the scale factor for both axes

$$\lambda = \frac{\Delta q}{\Delta w}. \tag{7}$$

The calculated λ is 0.9379 μm/pixel.

B. Image Processing

The image acquisition and processing is done by MATLAB/Simulink with cvLink toolbox in a computer. First, the color image is acquired by CCD camera in Fig. 3(a). For the convenience of processing as shown in Fig. 3(b), the acquired image is then converted into binary BW (black-and-white) version. Then, the exterior contour of microsphere in the BW image is extracted, and its center point is determined and marked in sequence as shown in Fig. 3(c) and (d).

IV. EXPERIMENTS

As shown in Fig. 4, the micropositioning device used in this research consists of two translation stages (PI M-111.1DG controlled by $Mercury^{TM}$ C-863 controller) and one rotary stage (SmarAct SR-3610-S controlled by MCS-3D controller). A video camera (AVT STINGRAY F-125C) and microscope lens (Opto zoom 70XL) are used as external sensor for 2D position measurement. Besides, a glass microsphere (Whitehouse Scientific, monodisperse particle standard) with measured size 200.9 μm is used as reference object.

Fig. 5 shows the flow chart of complete procedure of calibration and validation using camera. Considering the consuming time and number of parameters to be identified, we made 1081 measurements in trajectories of five squares taking 7 minutes for classical calibration to identify six parameters γ, L, τ, ζ, u_0 and v_0 where later three are depicted in Fig. 6. Afterwards, 72 measurement vectors were

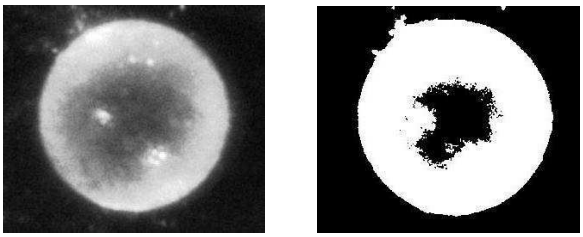

(a) Acquired image (b) Convert to BW image

(c) Find the contour (d) Mark the center

Fig. 3. Procedures of the image processing

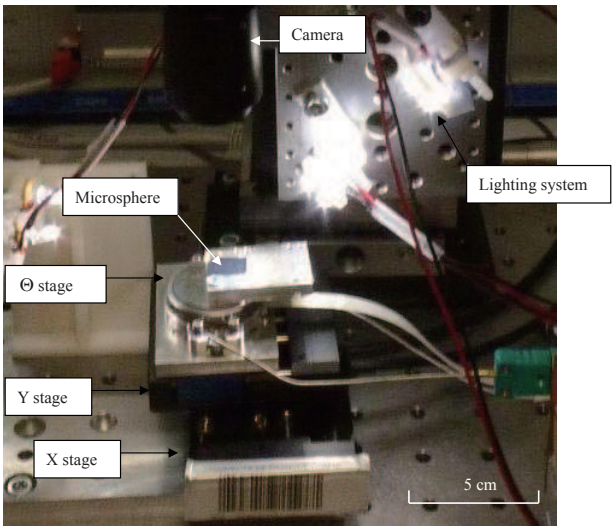

Fig. 4. Experimental setup for calibration and validation

made in about 15 minutes for self-calibration to identify three parameters γ, L and τ.

The position in robot workspace can be transformed into the image space through a rotation matrix R and a position vector w_0, with $w = [u, v]^T$ and $p = [x, y]^T$ describing the position vector of point in image space and robot space, respectively

$$w = \frac{1}{\lambda} Rp + w_0 \tag{8}$$

where

$$\begin{aligned} R &= Rot_z(\zeta) Rot_y(\pi) \\ &= \begin{bmatrix} -cos(\zeta) & -sin(\zeta) & 0 \\ -sin(\zeta) & cos(\zeta) & 0 \\ 0 & 0 & 1 \end{bmatrix}, \\ w_0 &= [u_0, v_0]^T. \end{aligned}$$

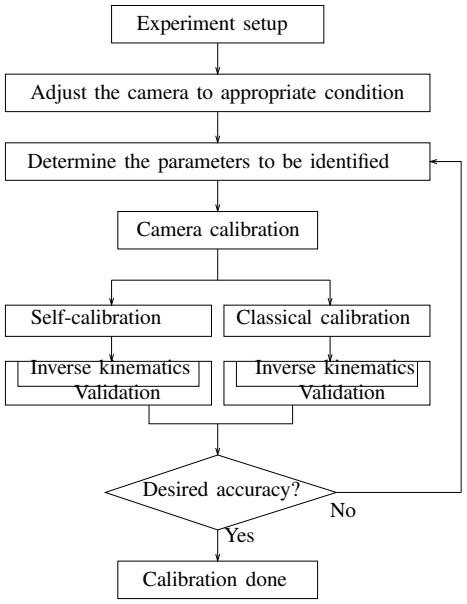

Fig. 5. Flow chart of calibration and validation for using camera

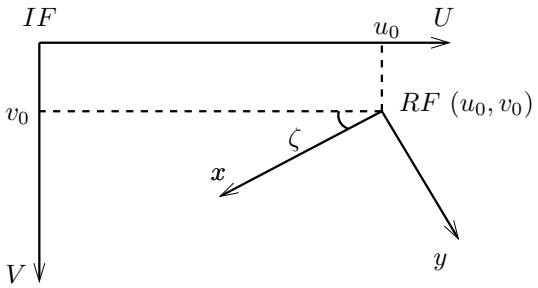

Fig. 6. Frames of image and robot. IF: image frame; RF: robot frame

A. Identification Results

Used DE algorithm, the identified values of parameters can be found in Table II and Table III. We can see that the identified γ, L and τ in self-calibration are quite different from those in classical calibration. The most different parameters are L and τ characterizing the position of the microsphere relative to the rotation center. That means the identification of both methods "see" different locations of the microsphere. One part of reasons is due to the optimization precision of the identification algorithm, which converge to a local minimum; another part is the environmental perturbation (e.g., thermal-induced drift) changing the location of the microsphere because two calibrations took place on two days.

TABLE II

IDENTIFIED RESULTS OF SELF-CALIBRATION USING 72 MEASUREMENTS

Identified parameters	Values
γ (rad)	-0.0096
L (μm)	86.9
τ (rad)	4.310

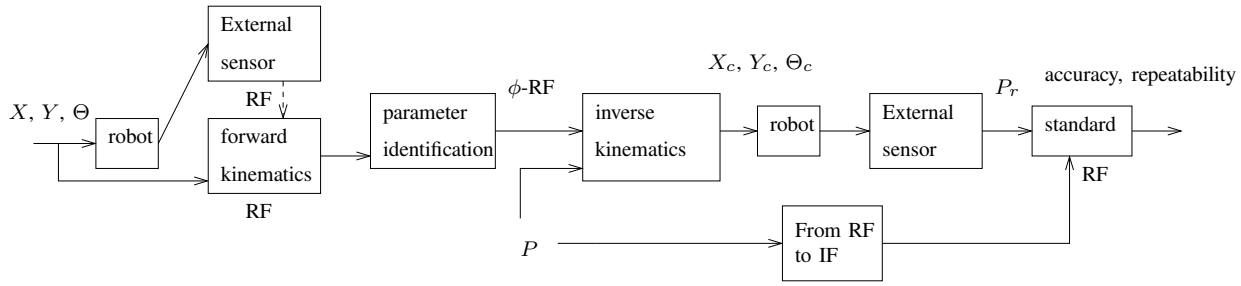

Fig. 7. Block diagram of the self-calibration and validation. IF: image frame; RF: robot frame

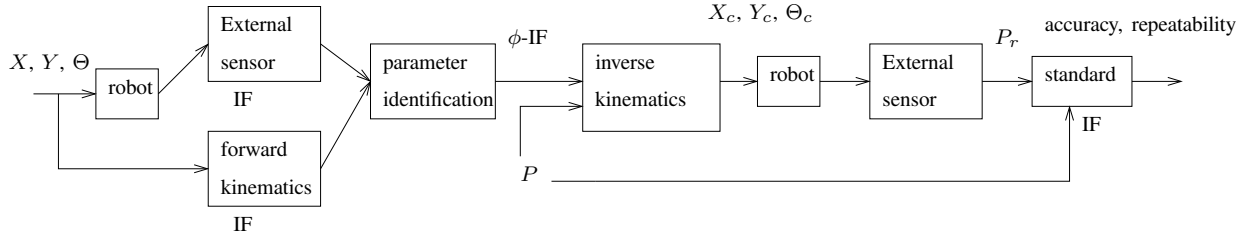

Fig. 8. Block diagram of the classical calibration and validation. IF: image frame; RF: robot frame

TABLE III

IDENTIFIED RESULTS OF CLASSICAL CALIBRATION USING 1081 MEASUREMENTS

Identified parameters	Values
γ (rad)	-0.006
L (μm)	17.027
τ (rad)	2.530
ζ (rad)	-0.025
u_0 (pixel)	841.093
v_0 (pixel)	157.548

TABLE IV

COORDINATES OF TEST POINTS FOR TWO CALIBRATIONS

Test points	self-calibrated model (μm)	classical model (pixel)
P_1	(200,150)	(500,350)
P_2	(360,270)	(340,470)
P_3	(360,30)	(340,230)
P_4	(40,30)	(660,230)
P_5	(40,270)	(660,470)

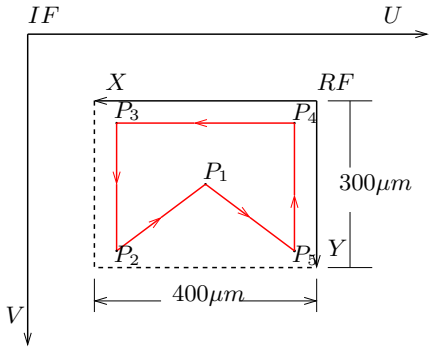

Fig. 9. Trajectory (red arrows) of performance tests for self-calibrated model. IF: image frame; RF: robot frame

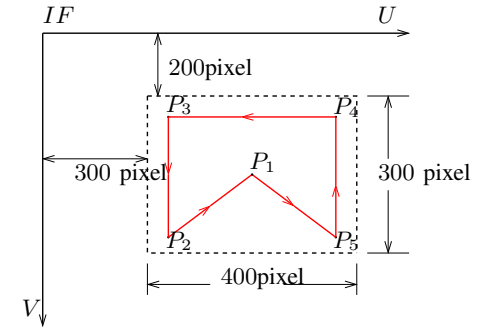

Fig. 10. Trajectory (red arrows) of performance tests for classical calibrated model. IF: image frame; RF: robot frame

B. Validation of Calibrations

To evaluate the accuracy achieved after calibrations, we performed validation experiments to both self-calibrated model and classical model resorted to ISO-9283 standard [7]. Fig. 7 and 8 are complete block diagrams of self-calibration and classical calibration as well as their validations. We can see that the main discrepancy between two processes is their reference frames in calibration phase. Self-calibration refers to RF and classical calibration to IF, so in validation phase, a transformation from RF to IF is necessary for self-calibration. Validations are implemented by computing joint coordinates via inverse kinematics and identified parameters. According to the measurement and calculation principle of the standard, five points (Table IV) in 2-dimensional workspace are defined for both tests, and the positioning accuracy and repeatability are computed by comparing the target positions and measured ones.

1) Self-Calibration: The test trajectories are shown (red arrows) in Fig. 9 with five points defined in RF. To evaluate the accuracy of the robot, the relationship between RF and IF should be known exactly, which is not an easy issue. In this case, the pixel-coordinates of the end-effector in 0° and 180° are recorded so as to be used to calculate the

position (the mean values in pixel) of the rotation center, which is the original point of RF. The orientation of x-axis is defined as the same as the positive motion orientation of the lower X stage. The y-axis is assigned perpendicularly to x-axis. Consequently the RF can be determined based on the hypothesis of no eccentricity. From Fig. 11, we can see that the repeatability is about 0.8 μm and the accuracy is around 3 μm for 5 test points. In a geometric point of view, the repeatability is the radius of the large circle; the accuracy is the distance from the center of small circle to the center of the square.

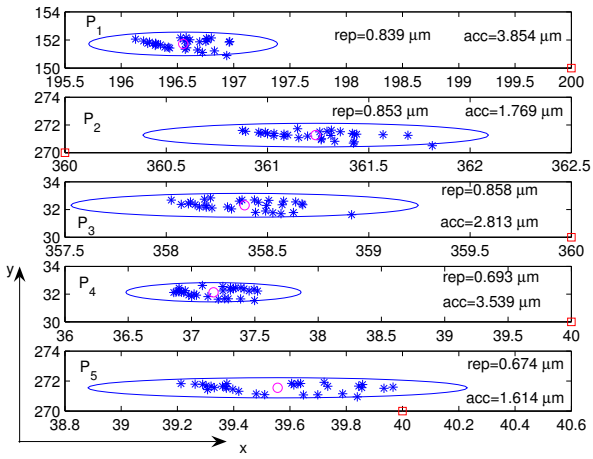

Fig. 11. Positioning accuracy (acc) and repeatability (rep) of self-calibration, x-axis and y-axis are in μm

2) Classical Calibration: The test trajectories with five points are defined in IF as shown in Fig. 10. The test results are given in Fig. 12, which show that the repeatability is about 0.5 μm and the accuracy is about 5 μm. This result show that the repeatability is better than self-calibration, but accuracy is worse.

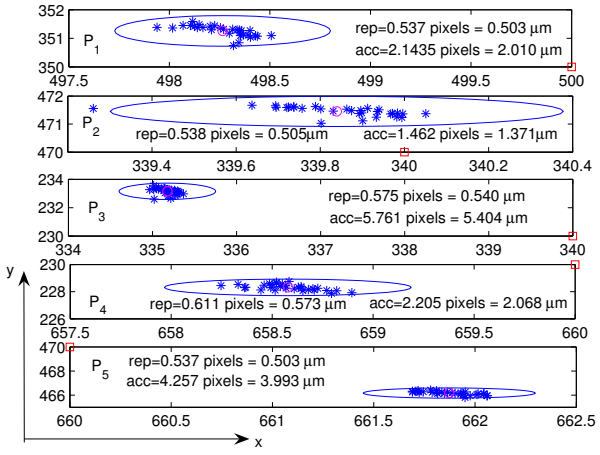

Fig. 12. Positioning accuracy (acc) and repeatability (rep) of classical calibration, x-axis and y-axis are in pixels

V. CONCLUSIONS AND FUTURE WORKS

This paper presented a full procedure of calibration and validation for 3-DOF $XY\Theta$ micropositioners which is used as coarse positioning to a microassembly platform. This work applies calibration methods at the macro scale to the micro scale, which could be termed as coarse calibration. To perform open-loop micropositioning for future automatic microassembly, this work is a necessary step. Differential evolution (DE) algorithm is applied due to identify the kinematic paramters. Based on a microscope vision system, experimental results show that the micropositioners have a repeatability is about 0.8 μm and the accuracy is around 3 μm by self-calibration. And by classical calibration, the repeatability is about 0.5 μm and the accuracy is about 5 μm. Hence, both calibrations achieve close performance and have their respective pros and cons in accuracy and repeatability. In order to suit microassembly tasks with rigorous accuracy requirements, the calibration should be improved. Such efforts will be conducted in our next step of research.

VI. ACKNOWLEDGMENTS

This work has partially been supported by the Franche-Comté region.

REFERENCES

[1] A.N. Das, R. Murthy, D.O. Popa, and H.E. Stephanou, A Multiscale Assembly and Packaging System for Manufacturing of Complex Micro-Nano Devices, *IEEE Transaction on Automation Science Engineering*, vol. 9, no. 1, 2012, pp 160-170.

[2] K. Rabenorosoa, S. Bargiel, C. Clévy, P. Lutz and C. Gorecki, Assembly of 3D Reconfigurable Hybrid MOEMS through Microrobotic Approach, *Lecture Notes in Automation, Frontiers of Assembly and Manufacturing*, 2010, pp 99-112.

[3] Bernhardt, R. and Albright, S., Eds. Robot Calibration. Chapman & Hall, 1993.

[4] Elatta, A., Gen, L., Zhi, F., Daoyuan, Y., and Fei, L. An Overview of Robot Calibration, *Information Technology Journal*, vol. 3, no. 1, 2004, pp. 74C78.

[5] J. M. Renders, E. Rossignol, M. Becquet, and R. Hanus, Kinematic Calibration and Geometrical Parameter Identification for Robots, *IEEE Transaction on Robot Automation*, vol. 7, no. 6, 1991, pp 721C732.

[6] A. Patel and K. Ehmann, Calibration of A Hexapode Machine Tool Using A Redundant Leg, *Int. J. of Machine Tools and Manufacture*, vol. 40, 2000, pp 48-512.

[7] ISO 9283:1998, *Manipulating Industrial Robots Performance Criteria and Related Test Methods*, 1998.

[8] D.J. Bennett , J.M. Hollerbach . Autonomous Calibration of Single-Loop Closed Kinematic Chains Formed by Manipulators with Passive Endpoint Constraints, *IEEE Transaction on Robotics and Automation*, vol. 7, no. 5, 1991, pp 597C606.

[9] R. Storn and K. Price, Differential Evolution - A Simple and Efficient Heuristic for Global Optimizaiton over Continuous Spaces, *Journal of Global Optimization*, vol. 11, no. 4, 1997, pp 341-359.

[10] W. Shang, S. Cong, and Y. Ge, Kinematic Self-Identification of a Redundantly Actuated Parallel Manipulator using Differential Evolution, *Proceedings of the 8th World Congress on Intelligent Control and Automation*, Jinan, China, 2010, pp 6654-6659.

[11] Q.S. Xu, Y.M. Li, and N. Xi, Design, Fabrication, And Visual Servo Control of An Xy Parallel Micromanipulator with Piezo-Actuation, *IEEE Transaction on Automation Science Engineering*, vol. 6, 2009, pp 710-719.

[12] L.S. Mattos and D.G. Caldwell, A Fast and precise Micropipette Positioning System based on Continuous Camera-Robot Recalibration and Visual Servoing, *in Fifth Annual IEEE Conference on Automation Science and Engineering*, Bangalore, India, 2009, pp 609-614.